ADSORPTION OF 4,6-DIMETHYLDIBENZOTHIOPHENE OVER *Cu/ZrO₂*

P. BAEZA[1],*, R. BASSI[2], M. VILLARROEL[2], J. OJEDA[3], P. ARAYA[4], G. AGUILA[4]

[1] Pontificia Universidad Católica de Valparaíso, Facultad de Ciencias, Instituto de Química, Casilla 4059, Valparaíso, Chile.
[2] Universidad de Santiago de Chile, Facultad de Química y Biología, Casilla 40, Correo 33, Santiago, Chile.
[3] Universidad de Valparaíso, Facultad de Farmacia, Casilla 5001, Valparaíso, Chile.
[4] Universidad de Chile, Facultad de Ciencias Físicas y Matemáticas, Departamento de Ingeniería Química y Biotecnología, Casilla 2777, Santiago, Chile.

ABSTRACT

The adsorption of refractory sulfur molecule 4,6-Dimethyldibenzothiophene (4,6-DMDBT) over copper supported on zirconia, using different copper loadings (2-10% w/w) and a zirconia support with a high specific surface area, was studied. The results showed that the adsorption capacity of 4,6-DMDBT over Cu/ZrO₂ increased with copper content, reaching a maximum at around 8% Cu (0.58 mmol 4,6-DMDBT per gram of adsorbent). The results of characterizations with H₂-TPR, Electrophoretic Migration, and XRD demonstrated that this Cu loading (8%) also corresponds to a maximum copper dispersion capacity for ZrO₂ support. Also, these absorbents showed considerable selectivity toward the adsorption of 4,6-DMDBT in a feed stream also containing Quinoline, decreasing adsorption capacity of 4,6-DMDBT by only 35%, despite both molecules being present in the same concentrations. The results of this work showed that desulfurization adsorption using Cu/ZrO₂ adsorbents can be an effective method to remove this type of refractory sulfur molecules, and an excellent alternative as a complementary process for deep desulfurization in the fuel industry.

Keywords: Desulfurization; Adsorption; Copper; Zirconia; 4,6-Dimethyldibenzothiophene.

1. INTRODUCTION

Due to the highly stringent environmental legislation on sulfur content in fuel, deep desulfurization has become an important subject for investigation. In this sense, and especially in the European Union, the "Euro V" standard for diesel fuel limits sulfur content to 10 ppm; elsewhere, in the United States, the fuel standard from the Environmental Protection Agency is the "Ultra Low Sulfur Diesel" (ULSD), which sets the maximum sulfur content at 15 ppm. These regulations require deeper desulfurization when encountering less reactive sulfur species. The purpose of removing the sulfur content from fuel is to reduce the sulfur dioxide (SO₂) emissions that result from using those fuels in motor vehicles, aircraft, residential and industrial furnaces, and other devices with fuel combustion. The presence of SO₂ and NOx produces "acid rain" and other emissions that are precursors of particulate matter in the atmosphere, resulting in an environmental impact.

In industry, the elimination of sulfur molecules present in fuel is carried out through a Hydrodesulfurization reaction (HDS). HDS uses bimetallic-supported catalysts, operates at elevated temperatures (400 – 600 ºC), and uses pressurized H₂ (100 – 200 atm). The HDS process can desulfurize compounds like Thiophene, Benzothiophene, and Dibenzothiophene, but it is unsuccessful in treating Dibenzothiophene derivatives that have alkyl groups near the sulfur atom, especially 4,6-Dimethyldibenzothiophene (4,6-DMDBT)[1,2]. This inability for treatment occurs since, for organic sulfur molecules with HDS catalysts, chemisorption takes place through the sulfur atom and depends strongly on the amount and types of substituents close to the S atom, which is characterized by a strong steric hindrance[3-5]. To desulfurize these "*refractory sulfur molecules*", a "*deep desulfurization*" is necessary. This catalytic process requires elevated temperatures and greater hydrogen consumption, and also causes a decrease in octane and cetane indexes.

There are several methods complementary to the HDS process. These include desulfurization by microbial oxidation[6,7], chemical oxidation[8,9], ultraviolet-assisted oxidation[10], biodesulfurization[11,12], and adsorption[13-17]. In the adsorption process, sulfur compounds are removed via p-complexation[18-22]. The competitive adsorption in a mixture of Dibenzothiophene (DBT) with Benzene shows greater selectivity toward the adsorption of organic sulfur compounds[13], and particularly towards adsorption of refractory compounds due to an enhanced ability for electron donation/back-donation[18,19].

In p-complexation, cations can form the usual s bonds with their s-orbitals, while their d-orbitals can back-donate electron density to the antibonding p-orbitals of the sulfur rings. The metals that can form this p-complexation are those that possess empty s-orbitals and available electron density at the d-orbitals[13,23], especially Cu(I) with an electronic configuration $1s^2 2s^2 2p^6 3s^2 3p^6 3d^{10} 4s^0$.

In preliminary studies, we showed that samples of Cu supported on zirconia possess significant adsorption capacity of sulfur compounds at relatively low copper contents. In particular, we studied the adsorption of Thiophene[23], Dibenzothiophene[13] and its derivative[24] from a mixture in n-octane at room temperature and atmospheric pressure. The results of these works showed that the adsorption capacity of copper on zirconia increases with the copper content, and higher capacities are observed in adsorbents treated with a flow of N₂O at 90ºC. This treatment generates a higher amount of Cu⁺¹ species, which are stabilized by acidic and redox properties of zirconia. Results showed adsorption capacities of 0.70 mmol of Thiophene[23], and 0.55 mmol of Dibenzothiophene, per gram of adsorbent[13] for a sample containing 6% Cu supported on zirconia calcined at 300 °C.

It is known that nitrogen content in petroleum varies depending on the source. At present, the composition of various petroleum derivatives indicates the predominance of highly alkylated nitrogen compounds[25-27]. Furthermore, the nitrogen compounds inhibit the HDS process and other hydrotreating reactions due to its preferential adsorption on the same catalytic sites[28-29]. It is clear that the nitrogen compounds are strong inhibitors of HDS reaction during hydrotreating processes, even at low concentrations[30]. Also, the organic nitrogen compounds are more resistant than sulfur compounds and require more severe reaction conditions. Due to the inhibiting effects among these compounds, simultaneous removal of sulfur, nitrogen, and aromatics represents a great challenge.

As a natural segue from the above, this study included adsorption experiments using a more refractory sulfur molecule, which was 4,6-Dimethyldibenzothiophene present in a mixture of n-octane under ambient conditions. In addition, in order to study the selectivity of these adsorbents, we show results of the competitive adsorption of sulfur and nitrogen compounds, 4,6-DMDBT and Quinoline (C₉H₇N), respectively, in adsorption experiments in which both molecules are present in the same feed stream.

2. MATERIAL AND METHODS

2.1 Adsorbent Preparation

The adsorbents were prepared by dry impregnation of zirconia with an aqueous solution of copper nitrate Cu(NO₃)₂·3H₂O (Merck p.a.), containing the required amount of salt to render copper concentrations of 2%, 4%, 6%, 8% and 10% (w/w). Zirconia was obtained by direct calcination of a commercial hydrous zirconium Zr(OH)₄ (MEL Chemicals) at 300 ºC for 3 h in a muffle furnace. After impregnation, the adsorbents were dried at 105 ºC for 12 h, and then calcined at 300 ºC for 3 h in a muffle furnace.

2.2 Adsorbent Characterization

The zirconia and the Cu/ZrO₂ adsorbents were characterized by

physical adsorption of N_2 in a Micromeritics ASAP 2010 equipment, after degasifying the samples at 200 ºC for approximately 1 h.

The fraction of zirconia surface covered by copper in different Cu/ ZrO_2 adsorbents was estimated using the electrophoretic migration (EM) technique using a Zeta Meter Inc. Meter, model 3.0, fitted with an automatic sample transfer unit. In each measurement, 30 mg of sample were suspended in 300 mL of solution 10^{-3} M of KCl, adjusting the pH with solutions of KOH or HCl 0.1 M, as required. In this way, we obtained the isoelectric point (IEP) of copper oxide and zirconium oxide, and the corresponding point of zero charge (PZC) of each adsorbent. The samples were used immediately after calcination, so that they would be in an oxidized state.

The crystal structure of the zirconium oxide and the different adsorbents was determined using a Siemens D-5000 diffractometer with Cu Ka radiation, a step of 0.02º and a step time of 3 s.

The adsorbent samples were studied with temperature programmed reduction (TPR) experiments in a 5% H_2/Ar stream in order to determine the different copper oxide species over the zirconia surface. In these experiments, 0.2 g of adsorbent was loaded in a quartz reactor and oxidized *in situ* in a 20 cm^3min^{-1} stream of pure O_2 at 300 ºC for 1 h. The reactor was cooled to room temperature and was purged for 30 min with pure Ar. The reducing mixture was introduced at 20 cm^3min^{-1} and heating started using a 10 ºCmin^{-1} temperature rate. The H_2 consumption was determined using a thermal conductivity cell.

2.3 Adsorption Experiments

Adsorption experiments were performed in a vertical Pyrex reactor equipped with a supporting glass porous disk. A bed of 500 mg of adsorbents was placed in the reactor and oxidized *in-situ* at 300 °C for 1 hour under a 20 mLmin^{-1} flow of pure O_2. After oxidation, the reactor was cooled down to room temperature and purged with pure Ar for 30 minutes. Then, a treatment was used to generate Cu^{+1} species over the zirconia surface[13,23]. This treatment consisted of reducing the oxidized sample entirely, treating it at 300 ºC for 1 hour under a 20 mLmin^{-1} flow of a 5% H_2/Ar mixture, cooling it down to 90 °C, partially reoxidizing with a 20 mLmin^{-1} flow of pure N_2O for 30 minutes, and cooling down to room temperature.

For the adsorption experiments, the feed stream was introduced into the reactor using a peristaltic variable flow pump. The experiment was performed using a solution of 2000 ppmw of 4,6-Dimethyldibenzothiophene (4,6-DMDBT) in n-octane (C_8H_{18}) at a feed rate of 0.5 cm^3min^{-1}. Samples were collected every 5 min, until adsorption capacity was achieved. For the selectivity study, experiments were performed using a mixture of 2000 ppmw of 4,6-Dimethyldibenzothiophene and 2000 ppmw of Quinoline in n-octane (C_8H_{18}), in order to check the competitiveness in the same conditions of adsorption experiments. Quinoline was chosen because it has a similar persistence and abundance in oil fields.

The samples were analyzed by gas chromatography – flame photometric detector (GC-FPD) using a Shimadzu GC-2010 equipped with an SPB-5 capillary column (L 30m, I.D. 0.25 mm, Film 0.25mm) given the following conditions: detector at 250 ºC, injector at 150 ºC, and 15 mLmin^{-1} (N_2) carrier flow. The column temperature was increased from 160 °C to 200 ºC at a rate of 40 °Cmin^{-1} and from 200 °C to 220 ºC at 5 °Cmin^{-1}. The sample (0.5 mL) was injected for each GC-FPD run, and the detection limit was 2 ppm.

3. RESULTS AND DISCUSSION

3.1 Specific Surface BET

In a previous study[13], it was observed that decreasing the calcination temperature produces an increase in the specific surface and pore volume of zirconia. Therefore, in this work the zirconia was calcined at 300 °C, with a specific area 293 m^2g^{-1}, higher value comparing to ZrO_2 calcined at 700 °C that has 36 m^2g^{-1}. Table 1 show the BET area and pore volume results for the commercial $Zr(OH)_4$, ZrO_2, and adsorbents systems of 4, 6 and 10% w/w Cu supported on ZrO_2. As previously reported[13], there was a slight decrease in specific area for all adsorbents independent of the copper load on the support. The decrease in specific area was, on average, approximately 10%. The pore volume did not change with the addition of Cu. Therefore, the decrease in the specific area was attributed to the increase in the copper content on the adsorbents.

Table 1: Specific area BET and porosity results of zirconia and 4, 6 and 10%Cu supported on ZrO_2 adsorbents. For comparison, the table includes the characterization of the commercial zirconium hydroxide (MEL Chemicals) used as precursor.

Sample	Nomenclature	BET Area (m^2g^{-1})	Pore Volume (cm^3g^{-1})
Commercial $Zr(OH)_4$	ZOH	400	0.22
ZrO_2 calcined at 300 ºC	ZrO_2	293	0.24
4%Cu/ZrO_2 calcined at 300 ºC	4%Cu/ZrO_2	258	0.24
6%Cu/ ZrO_2 calcined at 300 ºC	6%Cu/ZrO_2	238	0.24
10%Cu/ZrO_2 calcined at 300 ºC	10%Cu/ZrO_2	228	0.22

3.2 Electrophoretic Migration

The results of the zeta potential measurements, isoelectric point (IEP) of support and copper oxide, potential of zero charge (PZC), and fraction of surface covered by copper oxide (X_M), estimated from the adsorbent PZC and IEP of support and CuO, for the different Cu/ZrO_2 adsorbents are shown in Table 2. It can be seen that the values of the fractions of surface covered by CuO increase with the loading, reaching a maximum copper load of approximately 8% w/w. At higher levels of Cu content, the surface coverage did not increase, indicating that maximum copper dispersion ($X_M = 0.65$) on ZrO_2 is reached at loads close to 8% w/w Cu. Above this maximum Cu load, tridimensional copper species would begin forming.

Table 2: Results of zeta potential measurements: isoelectric point (IEP), potential of zero charge (PZC) and fraction of covered surface (X_M) for the different Cu/ZrO_2 adsorbents.

Sample	Cu load (% w/w)	IEP	PZC	X_M
CuO	-	10.07	-	-
ZrO_2	-	3.60	-	0.00
2%Cu/ZrO_2	2	-	4.31	0.11
4%Cu/ZrO_2	4	-	5.86	0.35
6%Cu/ZrO_2	6	-	6.89	0.51
8%Cu/ZrO_2	8	-	7.78	0.65
10%Cu/ZrO_2	10	-	7.82	0.65

3.3 X-ray Diffraction

Figure 1 shows the XRD diffractograms of the different Cu/ZrO_2 adsorbents. In all cases, low intensity and wide peaks of the diffraction pattern of the support were formed by a combination of tetragonal and monoclinic zirconia phases, which confirms our previous study[13]. When ZrO_2 is calcined at low temperatures, low crystallinity of the support is obtained. Also, no peaks corresponding to bulk CuO (or CuO with some crystallinity) were detected in adsorbents with copper content between 2% and 6%. However, when the Cu load is equal to or greater than 8% (8%Cu/ZrO_2 and 10%Cu/ZrO_2 adsorbents), a peak at q = 38.7º is clearly observed. This peak is characteristic of the tenorite structure of CuO. Thus, the formation of crystalline bulk CuO starts at a copper content of about 8%. Furthermore, at copper loads between 2% and 6%, the adsorbents only have CuO species that XRD analysis cannot detect, since these copper species are highly dispersed over the surface of ZrO_2 or, to a lesser extent, the CuO species are amorphous. However, as discussed later, in this range of copper content (2 to 6%), only highly dispersed CuO species was formed. Higher loadings of copper (8 and 10%) also produce the formation of bulk CuO, species that can be detected by XRD analysis. These results are in agreement with the results of electrophoretic migration.
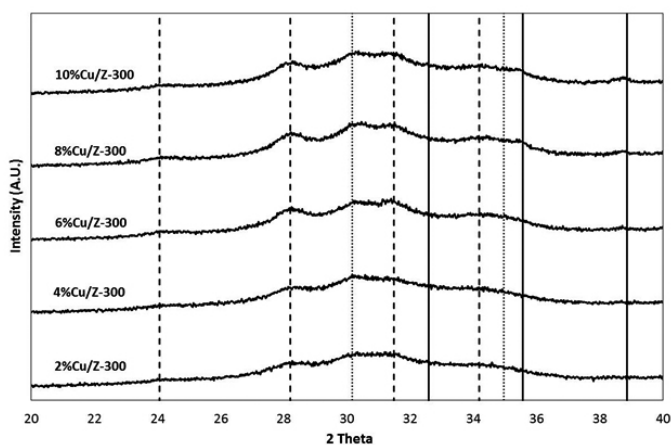
Figure 1: XRD results for Cu/ZrO$_2$ adsorbents with different copper loads. The characteristic diffraction lines of CuO (-), ZrO$_2$ monoclinic (---), and ZrO$_2$ tetragonal (…) are included.

3.4 Temperature Programmed Reduction by H$_2$

The TPR results of the adsorbents are shown in Figure 2. The adsorbent with the lowest Cu load, 2%Cu/ZrO$_2$, presents a broad peak centered at 270 ºC, with a maximum at 280 °C, which is associated with highly dispersed CuO species strongly interacting with the ZrO$_2$ support. As the Cu load was increased to 4%, the reduction peaks were displaced to lower temperatures due to the formation of highly dispersed species located on the surface having less interaction with the support. When the Cu load reached 6% (adsorbent 6%Cu/ZrO$_2$), two reduction peaks with temperature maxima close to 224 ºC and 236 ºC were clearly seen. These peaks are associated with the reduction of highly dispersed CuO species[13].
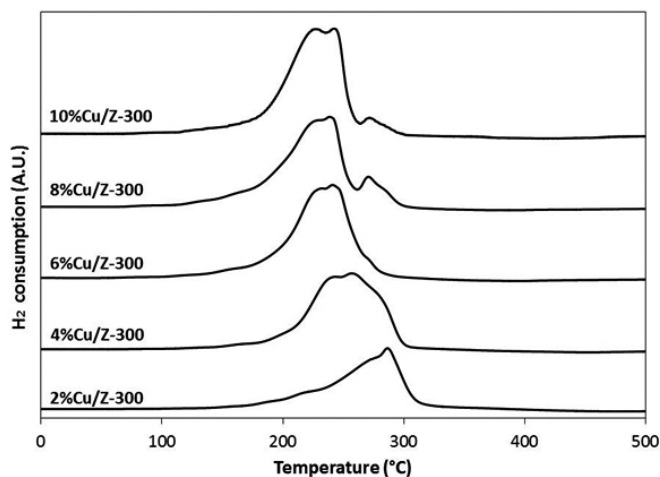

Figure 2: H$_2$-TPR results for Cu/ZrO$_2$ adsorbents with different copper loads.

At higher Cu loads, in adsorbents 8%Cu/ZrO$_2$ and 10%Cu/ZrO$_2$, a third peak with very low intensity appears at 266 °C, corresponding to the reduction of bulk CuO. This indicates that from a copper content of 8%, bulk CuO species begins to form. Therefore, TPR experiments are in agreement with both characterization techniques previously discussed (i.e., EM and XRD). It is important to observe that the appearance of bulk CuO species depends on the specific area of the ZrO$_2$. In this case, the results obtained with all the characterization techniques allow estimating that the dispersion capacity of ZrO$_2$ support is reached at Cu loading around 8% w/w, equivalent to 2.4 Cu atoms/nm^2 of ZrO$_2$. Below this dispersion capacity highly dispersed CuO species are formed, and above this limit bulk CuO species are formed.

3.5 Adsorption Tests

To determine the adsorption capacity of the samples, the fraction of adsorbed 4,6-DMDBT was used and the results were expressed as 1-(S_t/S_i), where S_t and S_i are the 4,6-DMDBT concentrations in time and in the initial sample (feed stream), respectively.

Initially, some adsorption experiments were performed using bare ZrO$_2$ samples. Also, samples of adsorbents oxidized with a pure O$_2$ flow of 20 mLmin^{-1} at 300 ºC for 1 hour (in order to obtain Cu^{2+}), or reduced with a 5% H$_2$/Ar flow of 20 mLmin^{-1} at 300 ºC for 1 hour (in order to obtain Cu^0) were used. The adsorption results of the above described samples showed no 4,6-DMDBT adsorption. Importantly, this behavior was consistent with results from literature, which indicate that Cu^{2+} and Cu^0 species supported on zeolite or zirconia do not have adsorption capacity via π-complexation[20,23]. Therefore, before adsorption experiments, all the adsorbents were pretreated to produce Cu^{+1} species, with the methodology previously indicated in the Adsorption Experiments section.

Figure 3 shows the 4,6-DMDBT adsorption curves for the different adsorbents used in this study. Clearly, the adsorption depends on the copper content present in each adsorbent. This behavior is more pronounced for low copper content levels supported on zirconia.
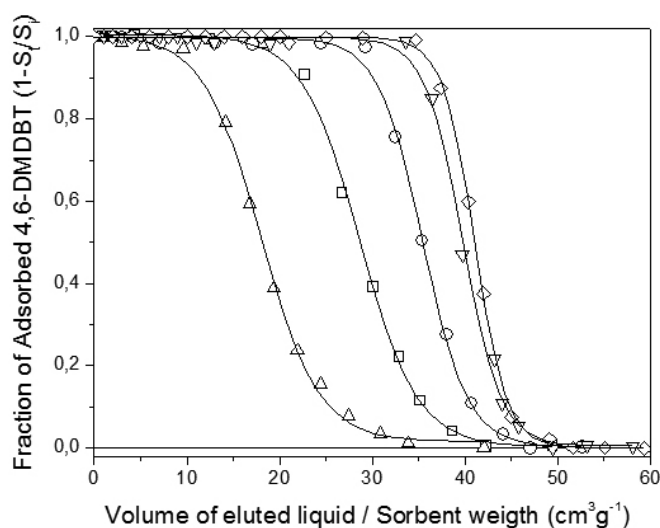

Figure 3: Fraction of adsorbed of 4,6-DMDBT on Cu/ZrO$_2$ with different copper contents, using a feed stream containing 2000 ppmw of 4,6-DMDBT in n-octane. (D) 2%Cu, (□) 4%Cu, (O) 6%Cu, (Ñ) 8%Cu, and (à) 10%Cu

The adsorption capacities can be estimated by integrating the area under the adsorption curves (Figure 3). These results are presented in Table 3 and show the adsorption capacity of 4,6-Dimethyldibenzothiophene (4,6-DMDBT) expressed as mmol 4,6-DMDBT per gram of adsorbent. The bare ZrO$_2$ (Z-300) has no adsorption capacity, as mentioned previously. In the case of adsorbents, the adsorption capacity reach a limit value of 0.58 mmol of 4,6-DMDBT per gram of adsorbent, and this value was reached at copper content of 8%. At higher copper loading (10%Cu), the adsorption capacity does not increase (0.59 mmol of 4,6-DMDBT per gram of adsorbent). In a previous work[13], considering 6%Cu/ZrO$_2$ adsorbent, a similar adsorption capacity was found for adsorption of DBT (0.55 mmol per gram of adsorbent). However, it should be noted that although the 4,6-DMDBT molecule is larger than the DBT, i.e. 4,6-DMDBT is more of a "*refractory sulfur molecule*", similar considerable adsorption capacities are achieved in this absorbent systems.

It should be expected that samples prepared with ZrO$_2$ calcined at 300 ºC can be prepared with a larger amount of copper, since only 65% of the surface is covered by copper (see Table 2). However, there is a high amount of dispersed copper in these samples prepared with ZrO$_2$ calcined at 300ºC. As shown in Figure 4, it can be concluded that adsorption of sulfurated molecules 4,6-DMDBT on Cu/ZrO$_2$ adsorbents is related to concentration and dispersion of Cu^{+1} surface species.

Table 3: Adsorption capacities of 4,6-Dimethyldibenzothiophene (4,6-DMDBT) for the different Cu/ZrO$_2$ adsorbents. (N.D. = not detected)

Adsorbent	Cu load (% w/w)	Cu load (atoms nm^{-2})	Adsorption capacity mmol 4,6-DMDBT (g of adsorbent)$^{-1}$
Z-300 support	-	-	N.D.
2%Cu/ZrO$_2$	2	0.6	0.28
4%Cu/ZrO$_2$	4	1.3	0.50
6%Cu/ZrO$_2$	6	1.9	0.54
8%Cu/ZrO$_2$	8	2.4	0.58
10%Cu/ZrO$_2$	10	3.0	0.59

Additionally, the selective adsorption of 4,6-DMDBT over Cu/ZrO$_2$ adsorbents was studied. For this objective, experiments were carried out with a feed stream that contained 4,6-DMDBT and Quinoline, in a mixture of 2000 ppmw of each molecule. Considering its higher adsorption capacity (see Table 3), 10%Cu/ZrO$_2$ absorbent was selected for these experiments. Figure 5 show 4,6-DMDBT adsorption curves from a feed stream containing 4,6-DMDBT and Quinoline. For comparison purpose, Figure 5 includes the 4,6-DMDBT adsorption curve when only 4,6-DMDBT was present in feed stream. As expected, the adsorption capacity of 4,6-DMDBT decreased when Quinoline was present, approximately by 35%. However, this decrease was not proportional to the amount of Quinoline, considering that both molecules were present in same concentrations.
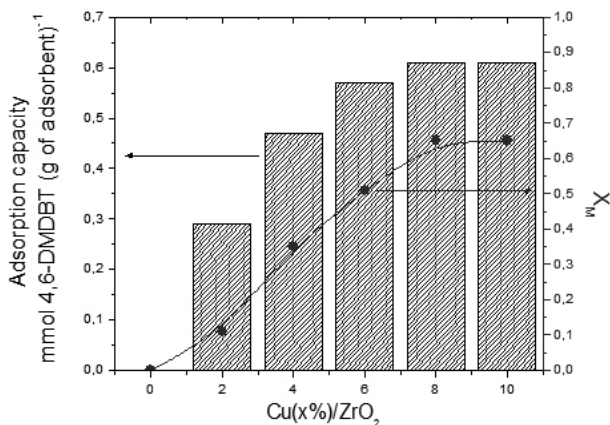

Figure 4: Adsorption of 4,6-DMDBT on Cu/ZrO$_2$ with different copper contents, in a feed stream containing 2000 ppmw of 4,6-DMDBT in n-octane (bar), and surface covered by metal X$_M$ (line).

In summary, this work demonstrated that copper supported on zirconia is a prominent adsorbent in the desulfurization of sulfur organic compounds and may have applications in deep desulfurization of fuel (adsorption of refractory sulfur molecules). The adsorption capacity of Cu/ZrO$_2$ system can be substantially improved by increasing the surface area of the zirconia, allowing higher concentration and dispersion of Cu^{+1} surface species.

4. CONCLUSIONS

The dispersed copper species supported on ZrO$_2$ in Cu^{+1} oxidation state have a high adsorption capacity for 4,6-DMDBT. Also, this adsorption capacity is proportional to the Cu content and its dispersion over ZrO$_2$. Based on characterization results, it was determined that ZrO$_2$ promotes stability and dispersion of Cu^{+1} surface species up to a copper content of 8%. Below this Cu loading (8%), high dispersion of copper on ZrO$_2$ is observed. Higher Cu loadings produce an agglomeration of the metal, i.e., bulk CuO species are formed.

Increasing the copper loading in adsorbents produce higher adsorption capacities for 4,6-DMDBT molecules. The maximum value of 0.58 mmol 4,6-DMDBT per gram of adsorbent is found when maximum dispersion capacity was obtained (Cu loading of 8%).

For 6%Cu/ZrO$_2$ adsorbent, the adsorption capacity of 4,6-DMDBT (0.54 mmol) is similar to that reported for DBT (0.55 mmol). Therefore, given that 4,6-DMDBT is one of the more refractory molecules of the HDS process, the adsorption desulfurization method is an effective complementary method to remove this type of molecule.

In addition, it was demonstrated that these adsorbents maintain selectivity for sulfur compound adsorption in the presence of nitrogen compound. The results show that 4,6-DMDBT was adsorbed even when Quinoline was present in the same feed stream.

The results of this work show that this type of Cu/ZrO$_2$ adsorbent was found to be an excellent alternative for a complementary process for deep desulfurization.
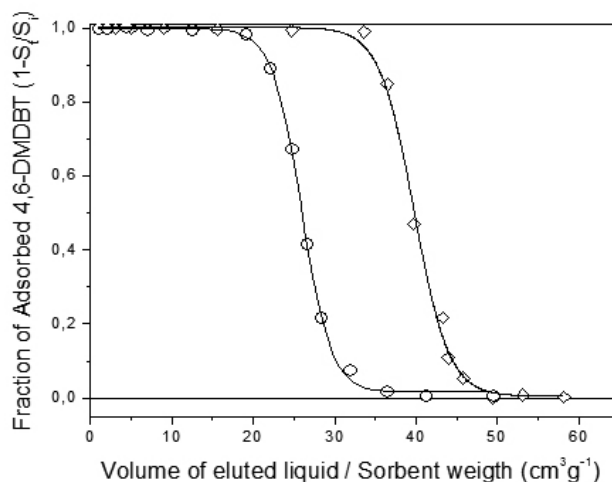

Figure 5: Fraction of adsorbed of 4,6-DMDBT on 10%Cu/ZrO$_2$, with a feed stream containing 2000 ppmw of 4,6-DMDBT in n-octane (à), and 2000 ppmw of 4,6-DMDBT and 2000 ppmw of Quinoline in n-octane (O).

In order to study the reusability of these adsorbents, regeneration of samples was carried out using pure O$_2$ at 300 ºC for 1 h after the first adsorption cycle. The results of adsorption after regeneration are shown in Figure 6. There, a slight decrease of the adsorption capacity for the 10%Cu/ZrO$_2$ regenerated adsorbent can be seen. The adsorption capacity decreased from 0.59 to 0.54 mmol of 4,6-DMDBT per grams of fresh and regenerated adsorbents, respectively.
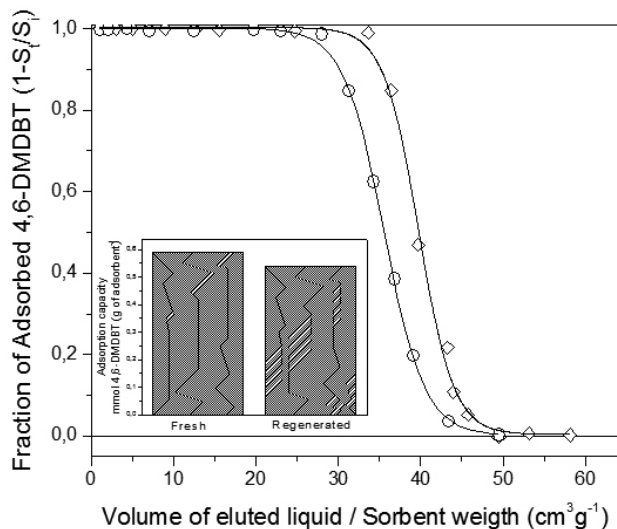

Figure 6: Fraction of adsorbed of 4,6-DMDBT on fresh 10% Cu/ZrO$_2$ (à), and adsorption of 4,6-DMDBT on regenerated 10% Cu/ZrO$_2$ (O). The insert are the adsorption capacities of fresh and regenerated adsorbent.

5. ACKNOWLEDGMENTS

6. REFERENCES

1.- A. Avidan, B. Klein, R. Ragsdale, Hydrocarb Process **80**, 47, (2001).
2.- Y. Gochi, C. Ornelas, F. Paraguay, S. Fuentes, L. Alvarez, J.L. Rico, G. Alonso-Núñez, Catal Today **107**, 531, (2005).
3.- E. Altamirano, J.A. de Los Reyes, F. Murrieta, M. Vrinat, J Catal **235**, 403, (2005).
4.- J.N. Díaz de León, M. Picquart, L. Massin, M. Vrinat, J.A. de los Reyes, J Mol Catal A-Chem **363**, 311, (2012).
5.- H. Nava, J. Espino, G. Berhault, G. Alonso-Nunez, Appl Catal **302**, 177, (2006).
6.- M. Grossman, in: M.L. Occelli, R. Chianelli (Eds.), Hydrotreating Technology for Pollution Control, Marcel Dekker Inc., New York, 1996, pp. 345.
7.- M. Ayala, R. Tinoco, V. Hernandez, P. Bremauntz, R. Vazquez-Duhalt, Fuel Process Technol **57**, 101, (1998).
8.- Y. Hangun, L. Alexandrova, S. Khetan, C. Horwitz, A. Cugini, D. Link, B. Howard, T.J. Collins, ACS Prep Div Petr Chem **47**, 42, (2002).
9.- V. Hulea, F. Fajula, J. Bousquet, J Catal **198**, 179, (2001).
10.- W. Lei, L. Shuzhen, C. Haijun, X. Yanyan, W. Xihui, C. Yujing, Fuel **94**, 165, (2012).
11.- M. Dinamarca, C. Ibacache-Quiroga, P. Baeza, S. Gálvez, M. Villarroel, P. Olivero, J. Ojeda, Bioresource Technol **101**, 2375, (2010).
12.- H. Zhang, G. Shan, H. Liu, J. Xing, Surf Coat Tech **201**, 6971, (2007).
13.- P. Baeza, G Aguila, G. Vargas; J. Ojeda, P. Araya, Appl Catal B-Environ **111**, 133, (2012).
14.- D.M. Ruthven, B.K. Kaul, Ind Eng Chem Res **32**, 2053, (1993).
15.- J. Weitkamp, M. Schwartz, S. Ernst, J Chem Soc Chem Comm **56**, 1133, (1991).
16.- W.W.C. Quigley, H.D. Yamamoto, P.A. Aegerter, G.J. Simpson, M.E. Bussell, Langmuir **12**, 1500, (1996).
17.- J. Yun, D. Choi, S. Kim, AICHE J, **44**, 1344, (1998).
18.- A.J. Hernández-Maldonado, R.T. Yang, Ind. Eng. Chem. Res. **42**, 123, (2003).
9.- A.J. Hernández-Maldonado, R.T. Yang, AICHE J. **50**, 791, (2004).
20.- A.J. Hernández-Maldonado, S.D. Stamatis, R.T. Yang, A.Z. He, W. Cannella, Ind Eng Chem Res **43**, 769 (2004).
21.- R.T. Yang, A.J. Hernández-Maldonado, F.H. Yang, Science. **301**, 79, (2003).
22.- A.J. Hernández-Maldonado, R.T. Yang, Catal Rev **46**, 111, (2004).
23.- P. Baeza, G. Aguila, F. Gracia and P. Araya, Catal Commun. **9,** 751, (2008).
24.- F. Aparicio, E Camú M. Villarroel, N. Escalona, P.Baeza, J. Chilean Chem. Soc. 58, Nº 4, 2057, (2013)
25.- P. Weng, D. Yu, B. Shi, B. Mu, and J. Que, ACS Prep. Div. Petr. Chem. **47**, 405, (2002).
26.- D. Yu, H. Xu, and J. Que, ACS Prep. Div. Petr. Chem. **47**, 128, (2002).
27.- G.C. Laredo, S. Leyva, R. Alvarez, M.T. Mares, J. Castillo, and J.L. Cano, Fuel **81**, 1341, (2002).
28.- P. Grange, Catal Rev Sci Eng **21**, 135, (1980).
29.- R.M. Koros, S. Bank, J. E. Hoffman, and M.I. Kay, ACS Prep Div Petr Chem **12**, 165, (1967).
30.- E. Furimsky, F.E. Massoth, Catal Today **52**, 38, (1999).